ACS OMEGA

Open Access

This article is licensed under CC-BY-NC-ND 4.0

http://pubs.acs.org/journal/acsodf

Article

Catalytic Deoxygenation of Palm Oil Over Iron Phosphide Supported on Nanoporous Carbon Derived from Vinasse Waste for Green Diesel Production

Phetcharat Nenyoo, Peerawat Wongsurakul, Worapon Kiatkittipong, Napat Kaewtrakulchai, Atthapon Srifa, Apiluck Eiad-Ua,* and Suttichai Assabumrungrat

Cite This: *ACS Omega* 2024, 9, 39757−39766

Read Online

ACCESS | Metrics & More | Article Recommendations

ABSTRACT: The vinasse waste was effectively converted to nanoporous carbon (NPC) via hydrothermal carbonization with potassium hydroxide (KOH) activation. The nanoporous carbon (NPC) exhibited a maximum surface area of 1018 m^2/g and it was utilized as a catalyst for the conversion of palm oil into green diesel fuel. The supported NPC catalyst was fabricated via a wet impregnation technique, where finely distributed iron phosphide (FeP) particles were cemented. The FeP/NPC catalyst was evaluated for its physicochemical characteristics using various techniques including X-ray diffraction (XRD), nitrogen sorption analyzer, transmission electron microscopy (TEM), and energy dispersive X-ray spectrometry (EDS) mapping. An investigation was conducted to examine the effects of different temperatures (ranging from 280 to 360 °C) on the conversion of palm oil through deoxygenation reactions. The FeP/NPC catalyst exhibited remarkable particle dispersion and surface area. At a reaction temperature of 340 °C, the FeP/NPC catalyst had the best selectivity for green diesel, reaching 68.5%. The finding implies that FeP catalysts, when supported, hold significant promise for converting triglycerides into renewable diesel fuel. Moreover, they provide the advantage of being more cost-effective than valuable metals, while demonstrating excellent catalytic efficiency in the production of biofuels. Furthermore, it has been shown that the FeP/NPC catalyst can be recycled by subjecting it to heat treatment to remove impurities and obtain reduction.

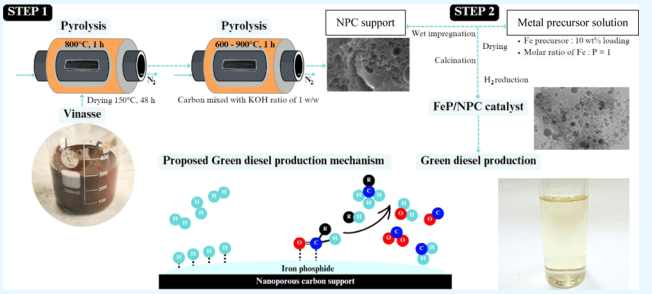

1. INTRODUCTION

The rising demand for petroleum, particularly diesel fuel, in the transportation and industrial sectors is driven by escalating economic requirements and the expanding worldwide population. The current scenario is resulting in a growing inclination toward converting waste biomass into an environmentally beneficial substitute for diesel derived from petroleum. Producing eco-friendly chemicals and biofuels from sustainable sources such as waste products and agricultural residues can mitigate the generation of greenhouse gas emissions by substituting fossil fuels.[1] Biodiesel, produced by chemically converting natural triglycerides such as plant oils and animal fats through a process called transesterification, is currently the most widely recognized form of biofuel. Nevertheless, the elevated oxygen concentration of biodiesel can result in problems such as heightened viscosity, a reduced freezing point, and diminished thermal stability, which can lead to challenges in engine systems.[2]

To overcome the limitations of biodiesel, extensive investigation is needed to explore technologies capable of transforming triglycerides into premium fuels that adhere to the criteria of petroleum diesel. Consequently, there is substantial research being conducted on alternate methods to convert vegetable oils and tallows into biohydrocarbons.[3,4] Catalytic deoxygenation is an efficient technology employed to enhance the quality of environmentally friendly fuel products, rendering them equivalent to conventional petroleum fuels. The process of catalytic deoxygenation, used in the manufacture of biofuels, usually employs systems that use hydrogen or do not require hydrogen. These systems operate within a temperature range of 250−420 °C. The process is aided by slightly acidic microporous or mesoporous heterogeneous catalysts under high pressure (10−100 bar).[5] This process consists of three simultaneous reactions: decarboxylation, decarbonylation, and hydrodeoxygenation. The impact of each reaction is contingent upon several elements, including

Received: May 27, 2024
Revised: August 27, 2024
Accepted: September 5, 2024
Published: September 10, 2024

© 2024 The Authors. Published by American Chemical Society

the catalyst type, reaction temperature, and hydrogen pressure.[6] The process of catalytic deoxygenation is employed to transform biomass feedstocks into environmentally acceptable fuels. The procedure frequently employs noble metal catalysts, such as palladium, platinum, and rhodium, that are supported on porous materials.[7] Nevertheless, the utilization of noble metals as catalysts is less cost-effective in comparison to transition-metal-based catalysts such as nickel, cobalt, iron, and molybdenum, particularly when considering large-scale commercial applications. Furthermore, it is imperative to address the crucial issue of low stability of noble metal catalysts during long-term operations.[8]

In recent years, researchers have investigated many options to replace noble metal catalysts in the process of deoxygenation. Some of these available are bimetallic catalysts,[9,10] metal sulfides,[11] metal carbides,[12,13] and metal phosphides,[14,15] all of which offer impressive catalytic performance, longevity, and cost-effectiveness. Nevertheless, some catalysts, like metal sulfides, might result in environmental damage as a consequence of the discharge of harmful sulfur agents.[16−18] Transition-metal phosphides have demonstrated exceptional catalytic efficacy in the conversion of triglycerides into biofuels, such as biojet fuel and green diesel. This is mainly due to their ability to minimize methanation, a secondary reaction that decreases the production of liquid hydrocarbons (LHC).[19] Their typical metallic and acidic catalyst behaviors allow them to offer multiple functions, effectively eliminating oxygen molecules. Although they have advantages, the investigation of their application for producing eco-friendly diesel from plant oils and animal fats has been restricted. Recent studies have demonstrated the potential of transition-metal phosphides, particularly those containing nickel, iron, and molybdenum, for the manufacturing of environmentally friendly diesel fuel.[20] These catalysts are cost-effective, provide superior stability, and display exceptional catalytic activity when compared to noble metals.[21,22] In addition, they exhibit excellent resistance to coking, strong mechanical durability, and high reactivity during the hydrodeoxygenation process.[23] Iron phosphide is acknowledged as a highly promising catalyst because of its exceptional activity, selectivity, and stability. The manufacturing of this substance utilizes inexpensive components and simple synthesis techniques, which make it suitable for efficient production on a wide scale. Although there are advantages, there is a scarcity of research on the utilization of iron phosphide catalysts for the removal of oxygen from vegetable oils in the creation of biofuels. Therefore, the objective of the study is to utilize an iron phosphide (FeP) catalyst in order to transform palm oil into environmentally friendly diesel fuel. Catalysts, which usually consist of a metal on materials with a large surface area, are essential in the deoxygenation process.[24] Porous materials such as alumina, silica, zeolites, and carbons function as catalyst supports, improving the dispersion and stabilization of metal nanoparticles. Nevertheless, support with elevated acidity levels can result in catalyst deactivation due to coking or carbon deposition.[25] Supports such as porous carbons, TiO_2, and ZrO_2, which have lower acidity, can prevent these problems while still maintaining a high surface area, which is crucial for an efficient catalyst support.[26,27] Porous carbon materials are utilized as a support for deoxygenation catalysts because they are cost-effective, environmentally friendly, and sustainable and can be customized in terms of porosity and surface chemistry. Porous carbons are particularly effective in distributing metal catalysts and exhibit impressive mechanical resilience under elevated temperatures and pressures.[28] They assist in the prevention of coking and enhance the efficient retrieval of precious metal catalysts. Recent studies highlight the use of carbon materials derived from waste as support for metal catalysts in deoxygenation.[29] Recent research emphasizes the utilization of carbon compounds obtained from waste as a means of supporting metal catalysts in the process of deoxygenation. Nevertheless, there has been a restricted amount of research conducted on the utilization of nanoporous carbon generated from waste biomass as a means to support metal phosphide catalysts for the purpose of deoxygenating palm oil in order to produce green diesel.[30] This research seeks to fill the gap in knowledge by exploring the use of industrial waste, notably vinasse waste from the sugar industry, as a support material for metal phosphide catalysts in the production of palm oil-based green diesel.[8,30,31]

Therefore, this study reported that a nanoporous carbon support was synthesized from vinasse waste using hydrothermal carbonization and activation with potassium hydroxide (KOH). The study investigated the effect of the activation temperature on the specific characteristics of nanoporous carbon. The selected nanoporous carbon was then used to support iron phosphide catalysts in palm oil deoxygenation. The synthesized iron phosphide catalysts were tested for their effectiveness in producing green diesel fuel with successful control over product selectivity achieved by tuning reaction conditions. The study also investigated the reusability of the iron phosphide catalyst on nanoporous carbon under optimal conditions for producing green diesel.

2. MATERIALS AND METHODS

2.1. Synthesis of Nanoporous Carbon (NPC). Vinasse waste, which was collected from the MitrPhol sugar factory located in Chaiyaphum, Thailand, was used as a raw material for the synthesis of nanoporous carbon. The vinasse was dried at 150 °C for 48 h in an oven, ground, and sieved into a powder. The preparation of nanoporous carbon (NPC) involved hydrothermal carbonization combined with activation using KOH (CARLO ERBA Reagents Co., Ltd., Paris, France) as an activating agent. Vinasse powder of 10 g was first pyrolyzed at an 800 °C ramp rate of 10 °C/min for 1 h under a nitrogen flow of 200 mL/min in a tubular furnace (Chavachote, Tube50/1009P, diameter = 10 cm). Then, carbon powder was mixed with a KOH ratio of 1 (w/w) for 15 min. The mixture of 10 g was activated at a temperature of 600, 700, 800, and 900 °C with a heating rate of 10 °C/min for 1 h under a nitrogen flow of 200 mL/min in a tubular furnace (Chavachote, Tube50/1009P, diameter = 10 cm). The residue on the NPC was washed with deionized water until neutral and dried in an oven at 105 °C for 24 h. The nanoporous carbon samples were denoted as NPC-X, where X represents the activation temperature of each sample. The physical and chemical properties of the vinasse powder and the NPC were characterized using thermogravimetric analysis (TGA) (Netzsch, TG 209 F3 Tarsus), energy dispersive X-ray analysis (EDX), X-ray fluorescence (XRF) (XRF, Rigaku, ZSX Primus IV), Fourier-transform infrared spectroscopy (FTIR) (PerkinElmer Scientific, Spectrum Two FT-IR Spectrometer), Brunauer−Emmett−Teller (BET) surface area analysis (Quantachrome Autosorp ASiQWin), and field emission scanning electron microscopy (FESEM) analysis (FEI, model Versa).

https://doi.org/10.1021/acsomega.4c05000
ACS Omega 2024, 9, 39757−39766

2.2. Synthesis of FeP/NPC Catalyst. Nanoporous carbon was used as a support material for the catalysts. The catalyst was prepared by following the incipient wetness impregnation method. Iron(III) nitrate nonahydrate [$Fe(NO_3)_3{\cdot}9H_2O$] 98% (CARLO ERBA Reagents Co., Ltd., Paris, France) was used as metal precursors. Diammonium hydrogen phosphate [$(NH_4)_2{\cdot}HPO_4$] (CARLO ERBA Reagents Co., Ltd., Paris, France) was used as phosphorus precursors. The iron phosphide is immobilized on nanoporous carbon by utilizing Iron(III) nitrate nonahydrate. The metal loading is precisely controlled at 10 wt %, and the phosphorus content is maintained at an initial molar ratio of 1.0 Fe/P. In the standard procedure, iron(III) nitrate nonahydrate was dissolved and stirred in deionized water. The solution was treated with diammonium hydrogen phosphate, and then nanoporous carbon particles were added. The mixture was maintained at a temperature of 100 °C for 48 h and then subjected to calcination at 800 °C. The calcination process involved heating the mixture at a rate of 10 °C per minute under a nitrogen flow of 200 mL per minute for a duration of 3 h. This was done using a tubular furnace (Chavachote, Tube50/1009P, with a diameter of 10 cm) in order to obtain the supported Fe−O−P polyphosphate complex species. Before further characterization and catalytic testing, the calcined sample (iron phosphate) was converted into iron phosphide by reduction under a hydrogen atmosphere. The calcined sample was reduced under a 20 mL/min hydrogen flow by heating from room temperature to 600 °C with a ramping rate of 10 °C/min for 6 h in a tubular furnace (Inner diameter = 10 mm, Outer diameter = 12 mm). The characteristics of prepared catalysts have been investigated by different techniques, such as X-ray diffraction (XRD, SmartLab, Rigaku, Japan), transmission electron microscopy (TEM, JEOL JEM-2100plus) equipped with an energy dispersive X-ray spectrometry (EDS), and N_2 adsorption/desorption isotherm.

2.3. Catalytic Deoxygenation of Palm Oil. The deoxygenation was conducted in a batch-type reactor with a volume of 100 mL. Palm olein oil, which serves as a feedstock, was procured from a local market in Thailand. The palm oil has the following fatty acid composition: The composition of the fatty acids in the substance is as follows: lauric acid (C12:0) 0.4%; myristic acid (C14:0) 0.8%; palmitic acid (C16:0) 37.4%; palmitoleic acid (C16:1) 0.2%; stearic acid (C18:0) 3.6%; oleic acid (C18:1) 45.8%; linoleic acid (C18:2) 11.1%; linolenic acid (C18:3) 0.3%; arachidic acid (C20:0) 0.3%; and eicosenoic acid (C20:1) 0.1%. According to deoxygenation test, 9 g of palm oil, 0.9 g of FeP/NPC catalyst, and 10 mL of dodecane (a solvent) were introduced into the autoclave. The system underwent a 15 min hydrogen purge to remove any air present in the reactor. The reactor was finally set with hydrogen at a pressure of 20 bar at the desired reaction temperatures of 280, 300, 320, 340, and 360 °C. The stirring speed was adjusted to 300 rpm, and the duration of the reaction was 3 h. The oil feed conversion refers to the transformation of triglycerides into other substances including intermediates and hydrocarbons. The product yields were calculated by analyzing the mass balance of liquid hydrocarbons in the products that corresponded to the oil feed. The formulas provided were used to compute the conversion of palm oil, the yield of liquid hydrocarbon (LHC), and the selectivity to green diesel (C15−C18).

$$\text{conversion of palm oil (\%)} = \frac{\text{oil in feed} - \text{oil in product}}{\text{oil in feed}} \times 100$$

$$\text{liquid hydrocarbons (LHCs) yield (\%)} = \frac{\text{mass of LHCs in product}}{\text{mass of oil in feed}} \times \text{conversion} \times 100$$

$$\text{selectivity of green diesel (\%)} = \frac{\text{green diesel in product}}{\text{oil converted}} \times 100$$

$$\text{green diesel yield (\%)} = [\text{LHCs yield (\%)} \times \text{selectivity of green diesel (\%)}]/100$$

For the characterization of the deoxygenation products, the gas chromatography-Flame Ionization Detector (GC-FID, 5890 SERIES II Plus) was used to analyze the products and determine the liquid hydrocarbon yield and composition of the resulting green diesel. The liquid hydrocarbon yield and selectivity of the green diesel are based on the reaction temperature.

2.4. Reusability of FeP/NPC Catalyst. To maintain the catalyst performance for reuse in subsequent recycling cycles, a regeneration procedure was implemented, which involves two crucial stages: cleaning and reduction. During the regeneration process, the catalyst that had been used was subjected to a temperature of 400 °C while being exposed to a N_2 flow of 20 mL/min for 3 h. This process removed any lingering impurities or carbon deposits that may have accumulated on the surface from the previous cycle. Afterward, the catalyst was subjected to a reduction in an environment of H_2 gas using flowing rate of 20 mL/min. The reduction occurred in a tubular furnace with an inner diameter of 10 mm and an outer diameter of 12 mm. The temperature was gradually increased at a rate of 10 °C/min until it reached 600 °C. The reduction process lasted 6 h. The purpose of this reduction phase was to restore the functionality of the active metal sites on the catalyst active sites, which may have been partially rendered inactive or oxidized during the previous reaction cycles.

3. RESULTS AND DISCUSSION

3.1. Characterization of Vinasse Powder and Physicochemical of Nanoporous Carbon. Figure 1 illustrates the temperature characteristics of the vinasse powder. The temperature-dependent mass loss profile within the temperature range of 30−900 °C. The whole mass reduction of

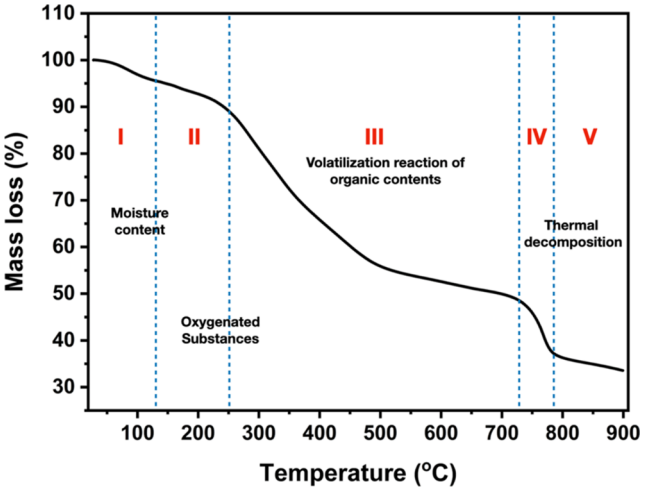

Figure 1. Thermal gravimetric analysis (TGA) of the vinasse powder.

https://doi.org/10.1021/acsomega.4c05000
ACS Omega 2024, 9, 39757−39766

vinasse powder can be categorized into five distinct steps. The initial decomposition stage involves the elimination of bound moisture and adhesive moisture and the evaporation of oxygenated substances, especially hydroxy compounds, within the temperature ranges of 30−120 °C and 120−250 °C, respectively. The second phase is characterized by significant volatilization of the organic content of vinasse, resulting in a mass loss of approximately 30%. Subsequently, there was a reduction in mass of approximately 5%, which was then accompanied by a decrease in weight of 10% due to thermal decomposition at the temperature range between 715 °C and 795 °C. Ultimately, there was no observed decrease in mass until reaching a temperature of 900 °C. The vinasse underwent decomposition under elevated temperatures, as seen in the TG profile: stages IV and V.

XRF analysis was utilized to determine the types and concentrations of oxide compounds present in vinasse powder. Based on the findings presented in Table 1, the dominant

Table 1. Oxide Compounds Composition of Vinasse Powder by XRF

no.	component	% mass
1	CaO	37.70
2	SO_3	30.00
3	K_2O	12.90
4	SiO_2	10.60
5	Cl	4.67
6	MgO	1.89
7	P_2O_5	1.00
8	others	1.24

oxide compounds in the powders were CaO and SO_3, accounting for 37.7 and 30.0% of the total mass of the vinasse powder, respectively. Additionally, smaller amounts of K_2O (12.9%), SiO_2 (10.6%), Cl (4.67%), MgO (1.89%), P_2O_5 (1.00%), and other compounds (1.24%) were also detected. XRF analysis revealed a significant presence of oxide compounds, indicating a high impurity level in the vinasse powder.

An EDX analysis was performed to ascertain the elemental composition of vinasse powder. Table 2 reveals that the

Table 2. Elemental Composition of Vinasse Powder by EDX

no.	element	% weight	% atomic
1	O	45.82	47.97
2	C	28.29	39.44
3	Ca	15.68	6.55
4	Si	4.83	2.88
5	Mg	2.25	1.55
6	S	2.05	1.07
7	other	1.08	0.54

powder mostly consisted of oxygen (O) and carbon (C), which accounted for 47.97 and 39.44% of the atomic composition, respectively. Furthermore, the vinasse powder had 6.55% calcium (Ca), 2.88% silicon (Si), 1.55% magnesium (Mg), 1.07% sulfur (S), and 0.54% other components. The analytical findings are consistent with the XRF results, verifying their consistency.

FTIR analysis was used to assess the surface chemistry of the vinasse powder in Figure 2. The wavenumber location and relative intensity of the FTIR spectra were utilized to assess the changes that occurred in the vinasse during hydrothermal carbonization under various conditions. Thus, the FTIR spectra profile of vinasse powder underwent notable alterations when compared to the profile of vinasse pyrolyzed at 800 °C. According to the FTIR analysis of vinasse powder, the observation in lignin is the stretching of aromatic −C═C− bonds, which occurs at a frequency of 1610 cm^{-1}, as seen in Figure 2a. This indicates the presence of hydroxyl and carbonyl functional groups of lignin in the lignocellulosic biomass of the vinasse powder, as anticipated from the vinasse feedstock. Additional lignin bands are also observed at 1373 cm^{-1}, which can be related to distortion of the aliphatic C−H bonds. The C−O vibrations associated with alcohols, phenols, and cellulose can be detected at approximately 1105 cm^{-1}. The vibrations occurring at approximately 600 and 850 cm^{-1} are associated with the bending of the C−H bonds. In contrast, the spectra below 500 cm^{-1} can be attributed to the vibration of inorganic substances.[32,33] The smooth vibration bands of NPC-900 were found due to the decomposition of lignocellulosic components during hydrothermal carbonization. Additionally, the KOH activation seems to successfully convert vinasse powder into nanoporous carbon, as seen in Figure 2b.[34]

Table 3 provides a summary of the textural pore structure of NPC support, including BET surface area, total pore volume, micropore volume, mesopore volume, and average pore diameter (D_{av}) obtained under several conditions. The optimal conditions for creating NPC as a metal catalyst support were attained by activating it at a temperature of 900 °C. The NPC demonstrated a surface area of 1018 m^2/g, a total pore volume of 0.836 cm^3/g, a micropore volume of 45.45%, a mesopore volume of 53.74%, and an average pore diameter of 3.285 nm under these conditions. The N_2 adsorption/desorption technique is frequently employed to characterize the pore structure of the NPC.[35] As seen in Figure 3, the NPC samples exhibit a unique combination of microporous and mesoporous structures, which are categorized by IUPAC as Type IV isotherms.[36,37]

In Figure 4, FESEM micrographs depict the external surface of the vinasse pyrolyzed and NPC-900 sample. The NPC-900 exhibits a distinct external surface with diverse pore cavities. Furthermore, the presence of internal cavities resembling a spongy matrix is evident, distinguishing it from that of the vinasse pyrolyzed sample. These surface and pore structures of NPC-900 indicate its promising potential as a catalyst support.

3.2. Characterization of FeP/NPC Catalyst. Figure 5a,b displays TEM images of the reduced FeP/NPC catalyst, revealing a well-dispersed arrangement of iron phosphide particles on the NPC support. The size of the iron phosphide particles increases as a result of the aggregation of metal particles on the NPC support.[20] Figure 6 displays a TEM image of the reduced FeP/NPC catalyst, along with EDS mapping of the elemental information. The image confirms that iron phosphide has been successfully loaded onto the NPC support and that the FeP crystals are uniformly dispersed inside a carbon framework.

The obtained iron phosphide on the NPC catalyst was analyzed using XRD diffraction, with measurements taken at the 2θ angle range of 30−70° in Figure 7. The XRD pattern of the FeP/NPC catalyst displayed a distinct peak with high intensity, indicating the presence of a crystalline phase. Within the 2θ angle range of 40−55°, the XRD pattern showed

https://doi.org/10.1021/acsomega.4c05000
ACS Omega 2024, 9, 39757−39766

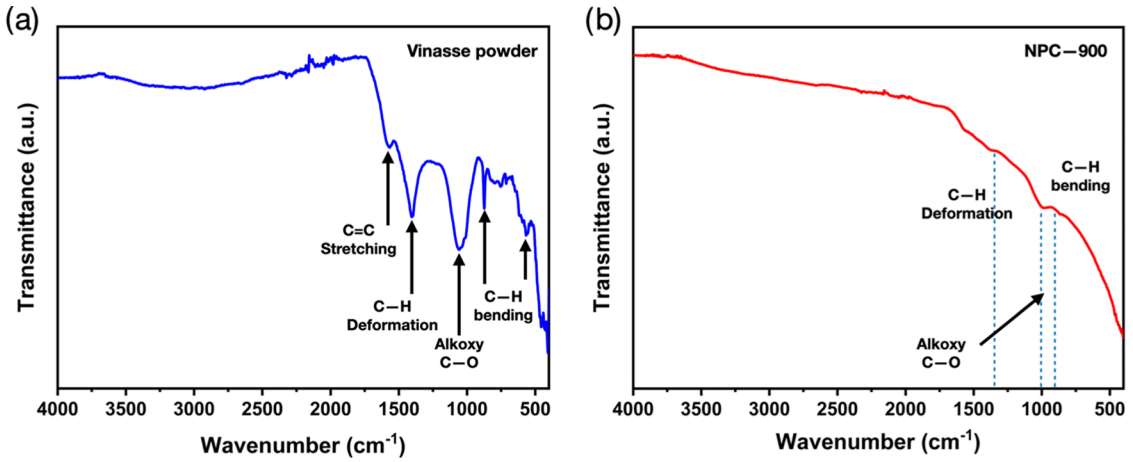

Figure 2. FTIR spectra of (a) Vinasse powder and (b) NPC-900 different..

Table 3. Pore Characteristics of Nanoporous Carbon (NPC)

conditions	pore characteristics				
	S_{BET} (m^2/g)	V_T (cm^3/g)	V_{mic} (%)	V_{mes} (%)	D_{av} (nm)
vinasse pyrolyzed 800 °C	72.02	0.074	0.54	67.43	4.144
NPC-600	671.60	0.525	29.33	52.19	3.130
NPC-700	620.50	0.475	28.11	48.57	3.061
NPC-800	558.50	0.451	17.10	49.20	3.233
NPC-900[a]	1018.00	0.836	45.45	53.74	3.285

[a]The highest porosity of NPC was applied as a metal catalyst support in palm oil deoxygenation.

overlapping diffraction lines, which can be attributed to the Fe_2P (PDF 85-1725) phase at 2θ angles of 42.0, 44.7, 46.8, and 51.7°, as well as the FeP (PDF 81-1173) phase at 2θ angles of 43.8 and 53.4°. This observation indicates that the Fe_2P phase underwent a conversion into FeP during the catalyst production procedure.[38] The increased temperature and extended duration during the preparation process likely influenced the ratio of metal to phosphorus by producing the partial liberation of phosphorus as a volatile substance, such as phosphine (PH_3), resulting in a change in phase.[20]

The BET surface area of the NPC support is 1018 m^2/g, with a total pore volume (V_T) of 0.836 cm^3/g, as shown in Table 4. The BET surface area of the decreased FeP/NPC

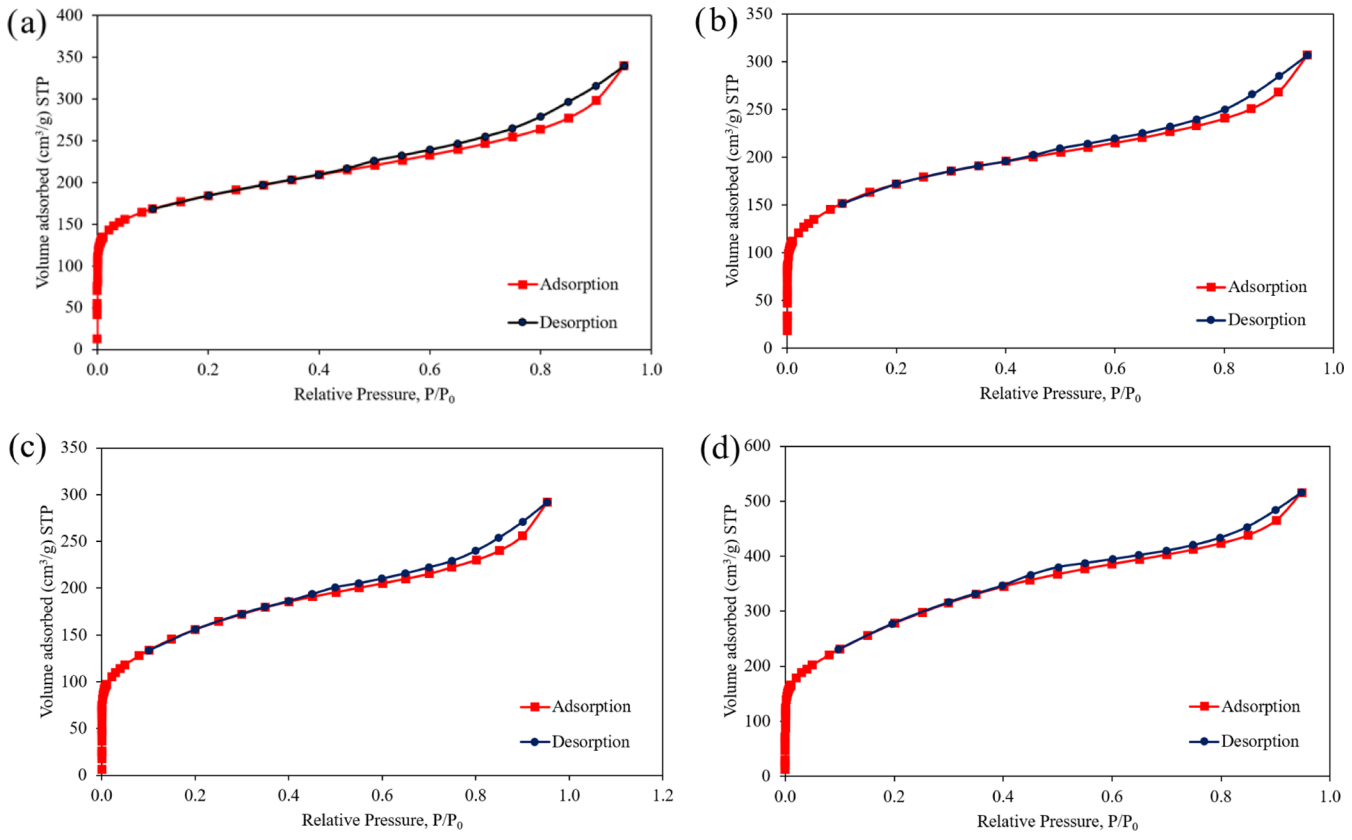

Figure 3. N_2 adsorption/desorption isotherms of NPC samples obtained at (a) 600 °C, (b) 700 °C, (c) 800 °C, and (d) 900 °C.

https://doi.org/10.1021/acsomega.4c05000
ACS Omega 2024, 9, 39757−39766

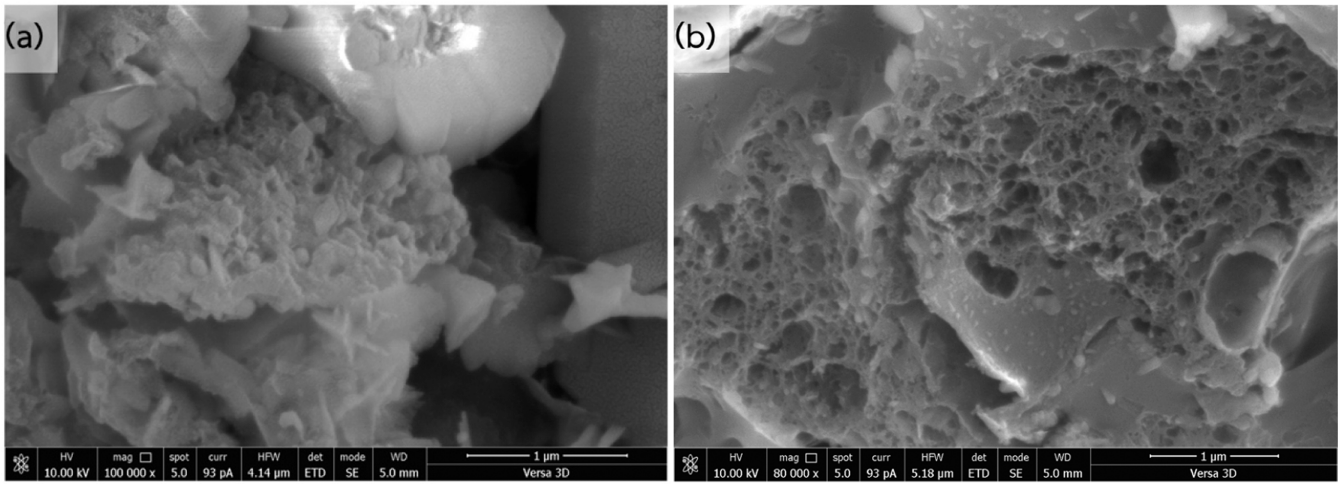

Figure 4. FESEM images of (a) vinasse pyrolyzed at 800 °C and (b) NPC-900 sample (supporting material).

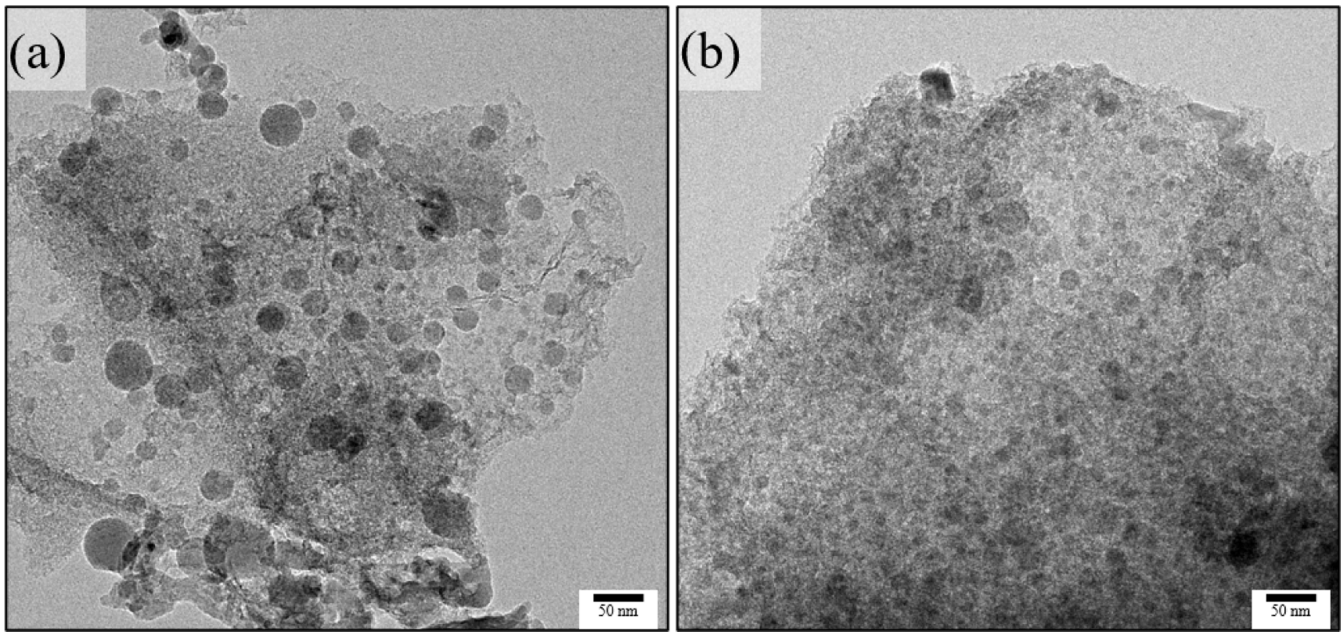

Figure 5. TEM images of the reduced FeP/NPC catalyst (a and b).

catalyst is 729.5 m^2/g, with a total pore volume (V_T) of 0.681 cm^3/g. Because metal particles are not present on the NPC surface, the adsorbed volume on supported FeP is less than that on the NPC support. Furthermore, the decrease in the surface area of the catalyst may be influenced by the mean particle size of the FeP catalyst due to aggregation during high temperature processing.[39]

3.3. Effect of the Deoxygenation Reaction Temperature. The effect of the deoxygenation temperature (280−360 °C) on the FeP/NPC catalyst was examined. Figure 8a depicts the effects of the deoxygenation temperature on palm oil conversion and liquid hydrocarbon output. Palm oil deoxygenation over the FeP/NPC catalyst results in full conversion at temperatures ranging from 340 to 360 °C. However, raising the deoxygenation temperature from 280 to 320 °C increased the conversion slightly from 78.2 to 93.1%, while decreasing the liquid hydrocarbon yield, possibly due to the high cracking reactivity at a higher reaction temperature. Asikin-Mijan[6] and Alsultan[31] found that lower deoxygenation temperatures resulted in lower conversion rates. In Figure 8b, the green diesel selectivity gradually improved from 34.1 to 68.5% as the reaction temperature climbed from 280 to 340 °C, but decreased at 360 °C, indicating the development of cracking activity.[40]

Figure 9 shows the hydrocarbon composition based on carbon number in green diesel fuels. As we are aware, palm oil feedstock primarily consists of unsaturated triglycerides, such as palmitic acid (C16:0, 37.8%) and oleic acid (C18:1, 45.8%).[20] Consequently, the main composition of oil palm feedstock would expect the major hydrocarbon products to be C_{16} and C_{18} hydrocarbons, aligning with the chemical composition of the oil feedstock. However, the FeP/NPC catalysts produced a product distribution primarily consisting of C_{15} and C_{17} hydrocarbons. The presented evidence indicates that the deoxygenation of palm oil using the respective catalysts primarily occurs through decarbonylation and decarboxylation reactions. However, it is noteworthy that hydrodeoxygenation also occurs concurrently, as evidenced by

https://doi.org/10.1021/acsomega.4c05000
ACS Omega 2024, 9, 39757−39766

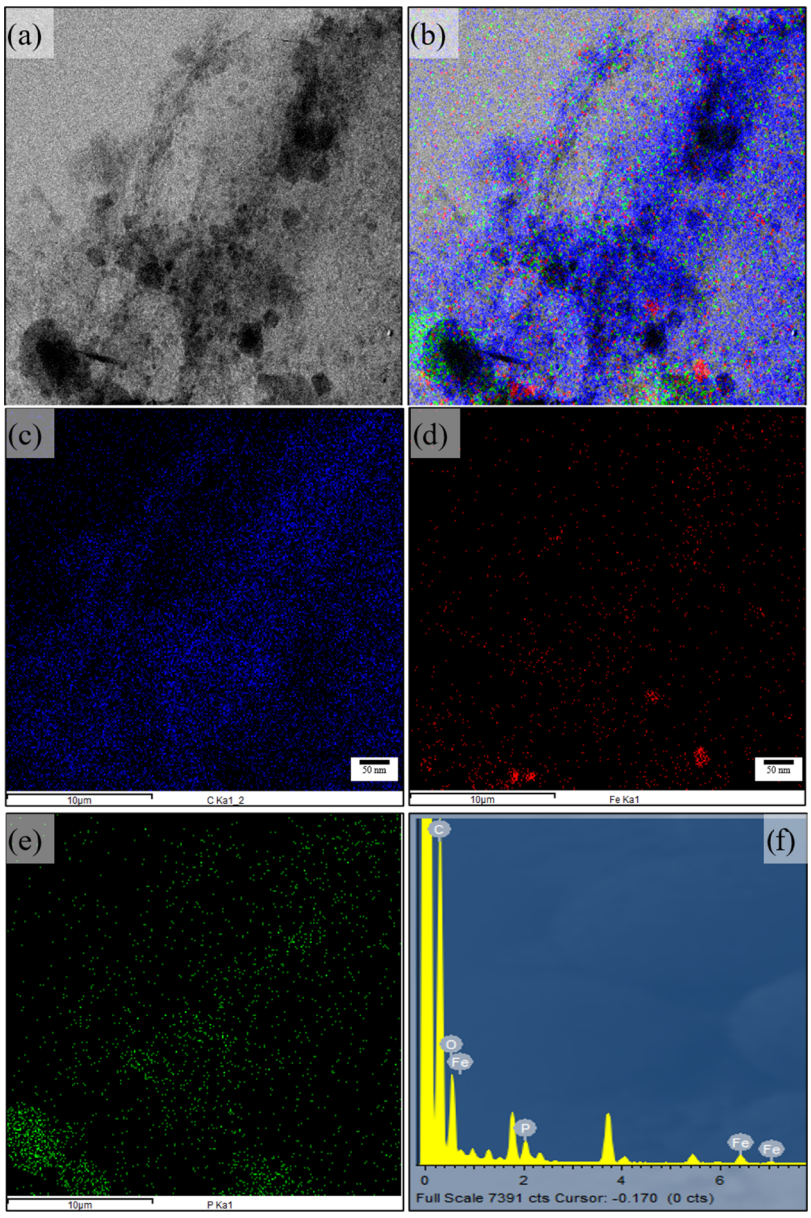

Figure 6. (a) TEM image and (b) EDS mapping of the FeP/NPC catalyst (c) C element, (d) Fe element, and (e) P element; and (f) the corresponding EDS spectrum.

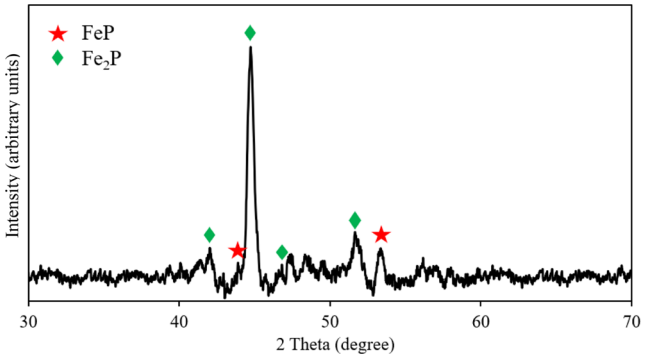

Figure 7. XRD pattern of the FeP/NPC catalyst.

the minor production of C_{16} and C_{18} hydrocarbons. The obtained result suggests that the DCO/DCO_2 reactions play a significant role in the deoxygenation of palm oil over the iron phosphide species.[41] This finding is attributed to the higher catalytic performance of the Fe−P catalyst, which facilitates the catalytic cleavage of C−O and C−C bonds, leading to the formation of C_{n-1} hydrocarbon.[20,30] Moreover, a recent study has further confirmed that the DCO/DCO_2 pathways are the preferred reactions for deoxygenation when utilizing iron phosphide catalysts.[42]

Table 4. Pore Characteristics of the FeP/NPC Catalyst

	pore characteristics			
catalyst	S_{BET} (m^2/g)	V_T (cm^3/g)	V_{mic} (%)	V_{mes} (%)
FeP/NPC	729.5	0.681	30.21	56.94

The reusability of the FeP/NPC catalyst was investigated via a deoxygenation reaction at a temperature of 340 °C, H_2 pressure of 20 bar, stirring rate of 300 rpm, and reaction time of 3 h. The green diesel yield indicates the proportion of green diesel obtained in relation to the total products. On the other

https://doi.org/10.1021/acsomega.4c05000
ACS Omega 2024, 9, 39757−39766

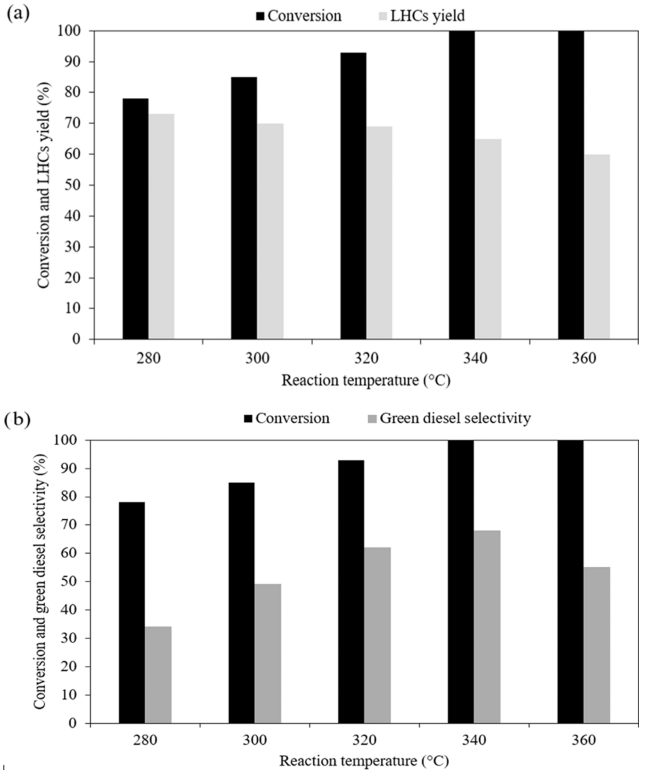

Figure 8. Effect of the deoxygenation reaction (DO) temperatures on (a) palm oil conversion, liquid hydrocarbon yield, and (b) selectivity to green diesel (C_{15}–C_{18}).

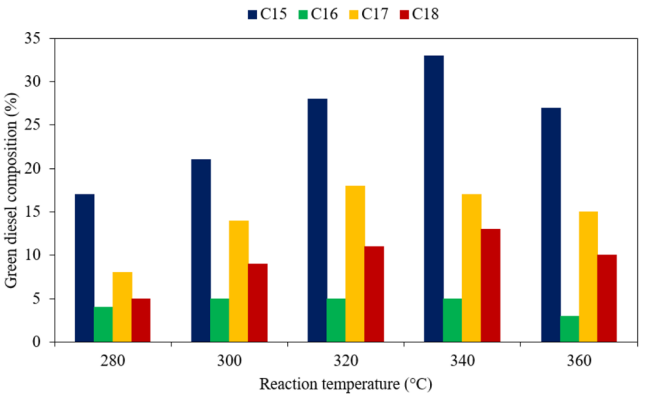

Figure 9. Green diesel composition based on carbon number obtained by using FeP/NPC catalyst.

hand, the recycling number demonstrates how many times the catalyst has been regenerated and reused during the process of producing green diesel.

In Figure 10, the green diesel yield diminishes slightly as the catalyst recycling number increases. First, at a recycling number of 0, the green diesel yield reached 44.2%, indicating a relatively high yield during the first use of the catalyst. However, as the catalyst underwent regeneration and was reused in subsequent cycles, the green diesel yield exhibited a downward trend. This decrease in green diesel yield with the recycling number can be attributed to the gradual deactivation of the catalyst over numerous cycles. The catalyst experiences harsh reaction conditions, such as high temperatures and exposure to various reactants, during the green diesel production process. These conditions can result in catalyst

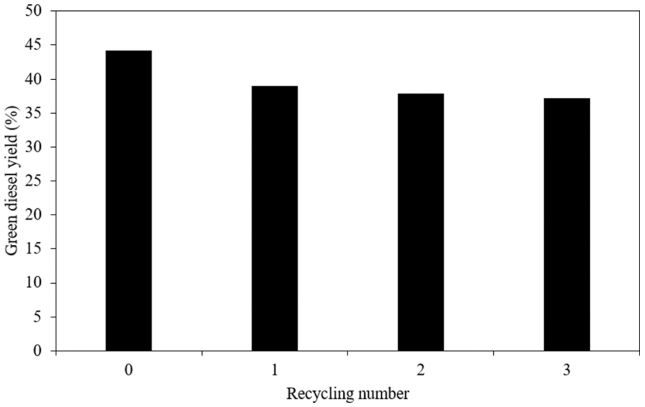

Figure 10. Reusability of FeP/NPC catalyst at a temperature of 340 °C, H_2 pressure of 20 bar, stirring rate of 300 rpm, and reaction time of 3 h.

fouling, deactivation, or even alterations in the catalyst's structure, thereby reducing its catalytic activity and selectivity of green diesel.[43] To preserve the catalyst activity and improve its reusability between each recycling cycle, a regeneration process was implemented consisting of two essential steps: decontamination and reduction.[44] Despite these regeneration efforts, the green diesel yields still exhibited a gradual decline as the recycling numbers increased, suggesting that the catalyst's reactivity and selectivity could not be completely restored to their original levels. The decline of green diesel yield could be ascribed to irreversible structural changes or the buildup of impurities on the catalyst, which might not be completely reversible through the regeneration process.[19]

4. CONCLUSIONS

Nanoporous carbon (NPC) derived from vinasse waste was successfully synthesized via two main processes, involving hydrothermal carbonization and KOH activation. The optimal condition for producing nanoporous carbon as a supporting material was achieved at an activation temperature of 900 °C and a KOH ratio of 1 (w/w). Under these conditions, the NPC support exhibited a maximum surface area of 1018 m^2/g, a total pore volume of 0.836 cm^3/g, a micropore volume of 45.45%, a mesopore volume of 53.74% and an average pore diameter of 3.285 nm. The internal cavities resemble a spongy matrix. The surface and pore structures of the NPC indicate its promising potential as a catalyst support. The catalyst exhibits a good dispersion of the iron phosphide particles on the NPC support, a successful iron phosphide loading on the NPC support, and a uniform dispersion of FeP crystals surrounded by a carbon framework. The high calcination temperature transformed the Fe_2P phase to FeP one which significantly exhibited high green diesel selectivity. The FeP/NPC catalyst produces mainly C15 and C17 hydrocarbons. This suggests that deoxygenation occurs through decarbonylation and decarboxylation reactions. The optimal condition identified in this study for the catalytic deoxygenation of palm oil into green diesel is a reaction temperature of 340 °C using the FeP/NPC catalyst, with a conversion of 100% and the highest green diesel selectivity of 68.5%. This study successfully demonstrated the regeneration and reusability of the FeP/NPC catalyst for green diesel production. The catalyst showed high green diesel selectivity, and Its reusability can be achieved after the regeneration process using heat treatment. The regenerated

https://doi.org/10.1021/acsomega.4c05000
ACS Omega 2024, 9, 39757−39766

catalyst is active for deoxygenation after 3 experimental runs, offering that FeP/NPC catalyst can be used as a potential alternative catalyst for producing green diesel. The result indicates the potential for cost-effective catalyst reuse in green diesel production, contributing to the progress in renewable energy initiatives.

AUTHOR INFORMATION

Corresponding Author

Apiluck Eiad-Ua − *College of Materials Innovation and Technology, King Mongkut's Institute of Technology, Ladkrabang, Bangkok 10520, Thailand;* orcid.org/0000-0002-2090-7334; Phone: +66-2-329-8300; Email: apiluck.ei@kmitl.ac.th; Fax: +66-2-329-8625

Authors

Phetcharat Nenyoo − *Bio-Circular-Green-Economy Technology & Engineering Center, BCGeTEC, Department of Chemical Engineering, Faculty of Engineering, Chulalongkorn University, Bangkok 10330, Thailand*

Peerawat Wongsurakul − *Department of Chemical Engineering, Faculty of Engineering and Industrial Technology, Silpakorn University, Nakhon Pathom 73000, Thailand*

Worapon Kiatkittipong − *Department of Chemical Engineering, Faculty of Engineering and Industrial Technology, Silpakorn University, Nakhon Pathom 73000, Thailand*

Napat Kaewtrakulchai − *Kasetsart Agricultural and Agro-Industrial Product Improvement Institute, Kasetsart University, Bangkok 10900, Thailand*

Atthapon Srifa − *Department of Chemical Engineering, Faculty of Engineering, Mahidol University, Nakhon Pathom 73170, Thailand;* orcid.org/0000-0002-9593-5014

Suttichai Assabumrungrat − *Bio-Circular-Green-Economy Technology & Engineering Center, BCGeTEC, Department of Chemical Engineering, Faculty of Engineering, Chulalongkorn University, Bangkok 10330, Thailand*

Complete contact information is available at: https://pubs.acs.org/10.1021/acsomega.4c05000

Author Contributions

Conceptualization: P.N., P.W., and A.E. Methodology: P.N. and P.W. Validation: W.K. Formal analysis: P.N., P.W., and N.K. Investigation: P.N. and P.W. Supervision: A.E. and S.A.. Writing-original draft: P.N. Writing-review and editing: N.K., A.S., W.K., S.A., and A.E. All authors have read and agreed to the published version of the manuscript.

Notes

The authors declare no competing financial interest.

ACKNOWLEDGMENTS

The authors acknowledge the Department of Chemical Engineering, Chulalongkorn University; the Material Analytical Instrument Service Unit (NMIS), College of Materials Innovation and Technology, King Mongkut's Institute of Technology Ladkrabang; the National Nanotechnology Center (NANOTEC), National Science and Technology Development Agency (NSTDA); and the Department of Chemical Engineering, Silpakorn University for their laboratory and facility financial support.

REFERENCES

(1) Ameen, M.; Azizan, M. T.; Yusup, S.; Ramli, A.; Shahbaz, M.; Aqsha, A. Process optimization of green diesel selectivity and understanding of reaction intermediates. *Renewable Energy* **2020**, *149*, 1092−1106.

(2) Zhao, C.; Lv, P.; Yang, L.; Xing, S.; Luo, W.; Wang, Z. Biodiesel synthesis over biochar-based catalyst from biomass waste pomelo peel. *Energy Convers. Manage.* **2018**, *160*, 477−485.

(3) Afshar Taromi, A.; Kaliaguine, S. Green diesel production via continuous hydrotreatment of triglycerides over mesostructured γ-alumina supported NiMo/CoMo catalysts. *Fuel Process. Technol.* **2018**, *171*, 20−30.

(4) Wang, F.; Jiang, J.; Wang, K.; Zhai, Q.; Sun, H.; Liu, P.; Feng, J.; Xia, H.; Ye, J.; Li, Z.; Li, F.; Xu, J. Activated carbon supported molybdenum and tungsten carbides for hydrotreatment of fatty acids into green diesel. *Fuel* **2018**, *228*, 103−111.

(5) Ameen, M.; Azizan, M. T.; Ramli, A.; Yusup, S.; Alnarabiji, M. S. Catalytic hydrodeoxygenation of rubber seed oil over sonochemically synthesized Ni-Mo/gamma-Al(2)O(3) catalyst for green diesel production. *Ultrason. Sonochem.* **2019**, *51*, 90−102.

(6) Asikin-Mijan, N.; Lee, H. V.; Abdulkareem-Alsultan, G.; Afandi, A.; Taufiq-Yap, Y. H. Production of green diesel via cleaner catalytic deoxygenation of Jatropha curcas oil. *J. Cleaner Prod.* **2017**, *167*, 1048−1059.

(7) Yoosuk, B.; Sanggam, P.; Wiengket, S.; Prasassarakich, P. Hydrodeoxygenation of oleic acid and palmitic acid to hydrocarbon-like biofuel over unsupported Ni-Mo and Co-Mo sulfide catalysts. *Renewable Energy* **2019**, *139*, 1391−1399.

(8) Asikin-Mijan, N.; Lee, H. V.; Taufiq-Yap, Y. H.; Abdulkrem-Alsultan, G.; Mastuli, M. S.; Ong, H. C. Optimization study of SiO2−Al2O3 supported bifunctional acid−base NiO-CaO for renewable fuel production using response surface methodology. *Energy Convers. Manage.* **2017**, *141*, 325−338.

(9) Itthibenchapong, V.; Srifa, A.; Kaewmeesri, R.; Kidkhunthod, P.; Faungnawakij, K. Deoxygenation of palm kernel oil to jet fuel-like hydrocarbons using Ni-MoS 2/γ -Al 2 O 3 catalysts. *Energy Convers. Manage.* **2017**, *134*, 188−196.

(10) Romero, A.; Nieto-Márquez, A.; Alonso, E. Bimetallic Ru:Ni/MCM-48 catalysts for the effective hydrogenation of d -glucose into sorbitol. *Appl. Catal., A* **2017**, *529*, 49−59.

(11) Srifa, A.; Faungnawakij, K.; Itthibenchapong, V.; Viriya-Empikul, N.; Charinpanitkul, T.; Assabumrungrat, S. Production of bio-hydrogenated diesel by catalytic hydrotreating of palm oil over NiMoS2/gamma-Al2O3 catalyst. *Bioresour. Technol.* **2014**, *158*, 81−90.

(12) Tran, C.-C.; Akmach, D.; Kaliaguine, S. Hydrodeoxygenation of vegetable oils over biochar supported bimetallic carbides for producing renewable diesel under mild conditions. *Green Chem.* **2020**, *22*, 6424−6436.

(13) Wang, F.; Xu, J.; Jiang, J.; Liu, P.; Li, F.; Ye, J.; Zhou, M. Hydrotreatment of vegetable oil for green diesel over activated carbon supported molybdenum carbide catalyst. *Fuel* **2018**, *216*, 738−746.

(14) Alvarez-Galvan, M. C.; Blanco-Brieva, G.; Capel-Sanchez, M.; Morales-delaRosa, S.; Campos-Martin, J. M.; Fierro, J. L. G. Metal phosphide catalysts for the hydrotreatment of non-edible vegetable oils. *Catal. Today* **2018**, *302*, 242−249.

(15) Berenguer, A.; Sankaranarayanan, T. M.; Gómez, G.; Moreno, I.; Coronado, J. M.; Pizarro, P.; Serrano, D. P. Evaluation of transition metal phosphides supported on ordered mesoporous materials as catalysts for phenol hydrodeoxygenation. *Green Chem.* **2016**, *18*, 1938−1951.

(16) Grilc, M.; Veryasov, G.; Likozar, B.; Jesih, A.; Levec, J. Hydrodeoxygenation of solvolysed lignocellulosic biomass by unsupported MoS2, MoO2, Mo2C and WS2 catalysts. *Appl. Catal., B* **2015**, *163*, 467−477.

(17) Wang, W.; Tan, S.; Zhu, G.; Wu, K.; Tan, L.; Li, Y.; Yang, Y. SDBS-assisted hydrothermal synthesis of flower-like Ni-Mo-S catalysts and their enhanced hydrodeoxygenation activity. *RSC Adv.* **2015**, *5*, 1−5.

(18) Zhang, Y.; Bi, P.; Wang, J.; Jiang, P.; Wu, X.; Xue, H.; Liu, J.; Zhou, X.; Li, Q. Production of jet and diesel biofuels from renewable lignocellulosic biomass. *Appl. Energy* **2015**, *150*, 128−137.
(19) Zhang, X.; Wu, J.; Zhu, L.; Wang, S. Novel Diesel-Like Liquid Fuel Production by Hydrodeoxygenation—In Situ Esterification of Lignin-Derived Bio-oil and Plant/Animal Oil. *Energy Fuels* **2023**, *37*, 2127−2133.
(20) Kaewtrakulchai, N.; Fuji, M.; Eiad-Ua, A. Catalytic deoxygenation of palm oil over metal phosphides supported on palm fiber waste derived activated biochar for producing green diesel fuel. *RSC Adv.* **2022**, *12*, 26051−26069.
(21) Bjelić, A.; Grilc, M.; Huš, M.; Likozar, B. Hydrogenation and hydrodeoxygenation of aromatic lignin monomers over Cu/C, Ni/C, Pd/C, Pt/C, Rh/C and Ru/C catalysts: Mechanisms, reaction microkinetic modelling and quantitative structure-activity relationships. *Chem. Eng. J.* **2019**, *359*, 305−320.
(22) Cecilia, J. A.; Infantes-Molina, A.; Rodriguez-Castellon, E. Hydrodechlorination of polychlorinated molecules using transition metal phosphide catalysts. *J. Hazard. Mater.* **2015**, *296*, 112−119.
(23) Griffin, M. B.; Baddour, F. G.; Habas, S. E.; Ruddy, D. A.; Schaidle, J. A. Evaluation of Silica-Supported Metal and Metal Phosphide Nanoparticle Catalysts for the Hydrodeoxygenation of Guaiacol Under Ex Situ Catalytic Fast Pyrolysis Conditions. *Top. Catal.* **2016**, *59*, 124−137.
(24) Aziz, I.; Sugita, P.; Darmawan, N.; Dwiatmoko, A. A. Synthesis of Green Diesel from Palm Oil Using Nickel-based Catalyst: A Review. *J. Kim. Valensi* **2023**, *9*, 59−75.
(25) Bhattacharjee, S.; Tan, C.-S. Hydrodeoxygenation of oleic acid in hexane containing pressurized CO 2 using Fe/SBA-15 as catalyst. *J. Cleaner Prod.* **2017**, *156*, 203−213.
(26) Cao, Y.; Shi, Y.; Liang, J.; Wu, Y.; Huang, S.; Wang, J.; Yang, M.; Hu, H. High iso -alkanes production from palmitic acid over bifunctional Ni/H-ZSM-22 catalysts. *Chem. Eng. Sci.* **2017**, *158*, 188−195.
(27) Srifa, A.; Kaewmeesri, R.; Fang, C.; Itthibenchapong, V.; Faungnawakij, K. NiAl2O4 spinel-type catalysts for deoxygenation of palm oil to green diesel. *Chem. Eng. J.* **2018**, *345*, 107−113.
(28) Hongthong, S.; Leese, H. S.; Chuck, C. J. Valorizing Plastic-Contaminated Waste Streams through the Catalytic Hydrothermal Processing of Polypropylene with Lignocellulose. *ACS Omega* **2020**, *5*, 20586−20598.
(29) Song, C.; Zhang, B.; Hao, L.; Min, J.; Liu, N.; Niu, R.; Gong, J.; Tang, T. Converting poly(ethylene terephthalate) waste into N-doped porous carbon as CO2 adsorbent and solar steam generator. *Green Energy Environ.* **2022**, *7*, 411−422.
(30) Miao, C.; Marin-Flores, O.; Davidson, S. D.; Li, T.; Dong, T.; Gao, D.; Wang, Y.; Garcia-Pérez, M.; Chen, S. Hydrothermal catalytic deoxygenation of palmitic acid over nickel catalyst. *Fuel* **2016**, *166*, 302−308.
(31) Alsultan, G. A.; Asikin-Mijan, N.; Lee, H. V.; Albazzaz, A. S.; Taufiq-Yap, Y. H. Deoxygenation of waste cooking to renewable diesel over walnut shell-derived nanorode activated carbon supported CaO-La 2 O 3 catalyst. *Energy Convers. Manage.* **2017**, *151*, 311−323.
(32) Callender, R.; Dyer, R. B. The dynamical nature of enzymatic catalysis. *Acc. Chem. Res.* **2015**, *48*, 407−413.
(33) Yang, X.; Ni, L. Synthesis of hybrid hydrogel of poly(AM co DADMAC)/silica sol and removal of methyl orange from aqueous solutions. *Chem. Eng. J.* **2012**, *209*, 194−200.
(34) Deng, H.; Li, G.; Yang, H.; Tang, J.; Tang, J. Preparation of activated carbons from cotton stalk by microwave assisted KOH and K2CO3 activation. *Chem. Eng. J.* **2010**, *163*, 373−381.
(35) Dizbay-Onat, M.; Vaidya, U. K.; Lungu, C. T. Preparation of industrial sisal fiber waste derived activated carbon by chemical activation and effects of carbonization parameters on surface characteristics. *Ind. Crops Prod.* **2017**, *95*, 583−590.
(36) Choi, G. G.; Oh, S. J.; Lee, S. J.; Kim, J. S. Production of bio-based phenolic resin and activated carbon from bio-oil and biochar derived from fast pyrolysis of palm kernel shells. *Bioresour. Technol.* **2015**, *178*, 99−107.
(37) dos Reis, G. S.; Wilhelm, M.; Silva, T. C. d. A.; Rezwan, K.; Sampaio, C. H.; Lima, E. C.; de Souza, S.M.A.G.U. The use of design of experiments for the evaluation of the production of surface rich activated carbon from sewage sludge via microwave and conventional pyrolysis. *Appl. Therm. Eng.* **2016**, *93*, 590−597.
(38) Adhikari, M.; Sharma, S.; Echeverria, E.; McIlroy, D. N.; Vasquez, Y. Formation of Iron Phosphide Nanobundles from an Iron Oxyhydroxide Precursor. *ACS Nanosci. Au* **2023**, *3*, 491−499.
(39) Wang, H.; Li, X.; Lan, X.; Wang, T. Supported Ultrafine NiCo Bimetallic Alloy Nanoparticles Derived from Bimetal−Organic Frameworks: A Highly Active Catalyst for Furfuryl Alcohol Hydrogenation. *ACS Catal.* **2018**, *8*, 2121−2128.
(40) Tsiotsias, A. I.; Hafeez, S.; Charisiou, N. D.; Al-Salem, S. M.; Manos, G.; Constantinou, A.; AlKhoori, S.; Sebastian, V.; Hinder, S. J.; Baker, M. A.; Polychronopoulou, K.; Goula, M. A. Selective catalytic deoxygenation of palm oil to produce green diesel over Ni catalysts supported on ZrO2 and CeO2−ZrO2: Experimental and process simulation modelling studies. *Renewable Energy* **2023**, *206*, 582−596.
(41) Zamani, A. S.; Saidi, M.; Najafabadi, A. T. Selective production of diesel-like alkanes via Neem seed oil hydrodeoxygenation over Ni/MgSiO3 catalyst. *Renewable Energy* **2023**, *209*, 462−470.
(42) Bui, P.; Cecilia, J. A.; Oyama, S. T.; Takagaki, A.; Infantes-Molina, A.; Zhao, H.; Li, D.; Rodríguez-Castellón, E.; Jiménez López, A. Studies of the synthesis of transition metal phosphides and their activity in the hydrodeoxygenation of a biofuel model compound. *J. Catal.* **2012**, *294*, 184−198.
(43) Ramanda, G. D.; Allwar, A.; Tamyiz, M.; Fatimah, I.; Doong, R.-a. Nickel/Biochar from Palm Leaves Waste as Selective Catalyst for Producing Green Diesel by Hydrodeoxygenation of Vegetable Oil. *Bull. Chem. React. Eng. Catal.* **2023**, *18*, 25−36.
(44) Arnosti, N. A.; Wyss, V.; Delley, M. F. Controlled Surface Modification of Cobalt Phosphide with Sulfur Tunes Hydrogenation Catalysis. *J. Am. Chem. Soc.* **2023**, *145*, 23556−23567.

https://doi.org/10.1021/acsomega.4c05000
ACS Omega 2024, 9, 39757−39766